Antarctic Research, Vol. 5, No. 1, 34～43, June 1994

The digital mapping produced with satellite image of the Zhongshan Station area in Antarctica

Sun Jiabing(孙家抦) and Gan Xinzheng(甘信铮)
Wuhan Technical University of Survey and Mapping, Wuhan 430070, China

Received March 11, 1994

Abstract Ice and snow dominat the land features in Antarctica. The great brightness and poorcontrast of ice and snow and streaking noise in satellite image make the procedure of image processing difficult. On the other hand however, the contrast between bare rock land/sea water and ice/snow is so high that the details of image will be overcompressed.

In the light of characteristics of satellite image in Antarctica, a filtering to remove streaking noise has been discussed. Based on automatic identify classification to enhance the details of objects and the method and theory of digital rectification of satellite image with ground control points measured from field survey are also presented.

Key words satellite image, streaking noise, direction filtering, image recognition, image enhancement, digital rectification, digital mapping.

1 Introduction

Antarctica is covered with ice and snow all the year round. The bad climate and adverse environment make ground surveying very difficult on Antarctic ice sheet. Therefore mapping with satellite images is a suitable approach. Such preliminary test with thematic mapper CCT data of Landsat-4 in the Zhongshan Station region is reported in this article. The altitude of Landsat-4 is 705 km, the inclination of orbit is 98°22′, satellite passes across the equator (descending node) at about 0930LT every day. But satellite passes above Zhongshan Station at about 0700～0800LT (descending orbit) or 1900～2000LT (ascending orbit) (Slater *et al.*, 1975).

The sun keeps rising in whole summer. Thus we can acquire satellite image data on this area under circumstance of ascending orbit or descending orbit. Because the station is located between 69 °20′ ～70 °20′S, about 80% of the images are overlapping with those of the adjacent orbit. Therefore the image can be acquired from 5 neighbouring orbits for the same area. In addition, both Landsat-4 and Landsat-5 are working, thus there are more chances of acquiring the image in this area than in the equator. In the Antarctic region the weather is changing all the time and we hardly have a fine day. Moreover the satellite image covers the area once in 16 days. Here the images gained on January 20, 1989 were used for the experiment. The orbit numbers is 124/109, covering the area of latitude 68°35′～70°35′S and longitude 74°45′～80°50′E along the satellite orbit in a four-sideline range.

TM is a sensor of multi- spectrum scanning imagery, which has been loaded at Landsat 4/5 called the Thematic Mapper. The resolution is 30 m (after the rough processing, the size of a pixel is 28.5 m × 28.5 m). Each single band image has been recorded on CCT (computer compatible tape), the size is 5965 line × 6968 pixel. The total amount is divided into seven bands, with the length of bands ranging from 0.45 to 12.5 μm, the length of wave for each band is shown in Table 1.

The TM data used in the experiment was provided by the EOSAT Company. Only the rough processing had been made by using the attitude data from the satellite. The deformation arises from the earth rôtation, the residual error remained to be large, and the subdivision of image has still been made along the tralking direction. Therefore the geometrical collection should be made and certain map projection should be used when mapping is needed. On the radiation aspect, the streaked noise caused by the respond movement of the scanner made image enhancement and mapping difficult. On the other hand, in Antarctica bright ice and snow led the image with low contrast. But the contrast between the small bare rock, sea water and ice/snow is much large. So the conventional approach is of no use, therefore some special methods have been introduced.

Table 1. Wave length range of TM image bands(Slater *et al.*, 1975)

Passage	Wave length range(μm)	Display speciality
TM1	0.45～0.52	Brightness value of snow and ice is 255, boundary between ice-snow and bare rock, sea water is clear.
TM2	0.52～0.60	Snow topography is slightly visiable, there are differences between thin float ice and sea water.
TM3	0.63～0.69	Snow topography is displayed better, there are differences between ice and snow.
TM4	0.76～0.90	Snow topography is shown well, there are obvious differences between land ice and sea ice.
TM5	1.55～1.75	There are obvious differences between bare rock and water, between bare rock and ice/snow, dissolved snow are clearly shown.
TM6	10.4～12.5	Snow surface showing the variation of temperature in layers.
TM7	2.08～2.35	Similar with TM 5

2 Removal of streaking noises

In scanning the responding deviations of sensor brought about streaking noises in the shape of comb. Through measurement, on image the brightness disparate values are 1～3 (whole image brightness range between 0 to 255). Due to various ground scenes in a great part of the earth, such deviations are negligible, but the ground objects are monotonous in Antarctica, therefore, they are quite obvious especially after the enhancement of image. In entire image the noises are distributed unevenly with different shades, there are streaking noises in some area and there are no ones in other area. If the noises have not been removed, many streaking noises would be arranged on the final mapping. In spite of this, the streaking noises are regularly arranged. They are identical

with the scanning direction; on the other hand, they are dark-colored on the left, but light-colored on the right. Therefore, for the partial noise area we can use direction filtering method to remove the noises (Gonzalez and Wintz, 1977). The process is as follows: if ideal image's function for $f(x, y)$, through the Fast Fourier Transform counting to get the space frequency domain image's function for $F_i(u,v)$:

$$F_i(u,v)=F(f(x,y)) \tag{1}$$

where, F is Fourier Transform symbol.

This time image's noises occur at a direction (shown in Fig. 1), so we consider to

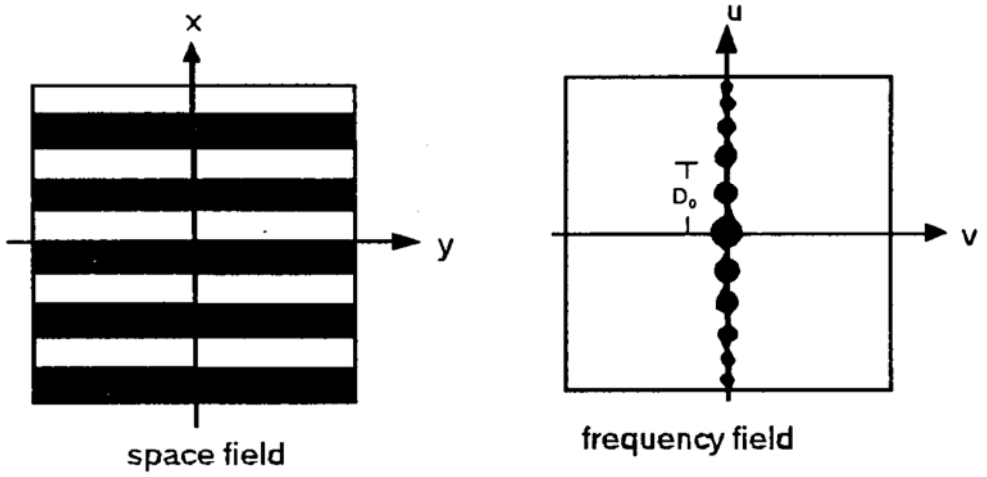

Fig. 1. The images in two different fields.

make use of direction filtering method.

The image's function of inclusive streaking noise for $g(x,y)$

$$g(x,y)=f(x,y)+n(x,c) \tag{2}$$

then

$$\begin{aligned} G(u,v)&=F[g(x,y)]\\ &=F[f(x,y)+n(x,c)]\\ &=F_i(u,v)+N(u,o) \end{aligned} \tag{3}$$

after filtering

$$\begin{aligned} F_i'(u,v)&=G(u,v)-N(u,o)\\ f'(x,y)&=F^{-1}[F_i'(u,v)]\\ &=F^{-1}[G(u,v)-N(u,o)] \end{aligned} \tag{4}$$

supposed noise function for $n(x,c)$. Adopting the filtering method is good use for the removel of noises. The streaking noise is removed almost entirely which paves the way for the enhancement of image.

3 Image enhancement based on automatic recognition

The colouring satellite images, if necessary, are composed of three bands. TM provided seven band's images. As a result of observation and measure, images on the monitor of computer are displayed. Each band's comfiguration of the earth's surface are expressed as shown in Table 1. According to the characteristics listed in Table 1, the satellite images of Antarcitc area are depicted. It seems better to select TM 4, 3 and 2 bands, but the large part of Antarctic area is ice sheet and snowfield. The reflex brightness is over bright. Between the same kind of ground objects, the contrast is small. However, between different kind of ground objects the contrast is over large. For example, TM4 statistical histogram of image in Zhongshan Station is shown in Fig. 2 (a). It is thus clear that the brightness of ice and snow are large, the frequency is high, the contrast is small. In comparison of the brightness of sea water, bare rock and some thin floating ice in the sea with that of ice and snow the contrast is over large. If the brightness of ice/snow stretches to both the high/low directions as shown in Fig. 2(b). Though snow's contrast has enhanced, other ground objects contrast and brightness are all very small. On the optical image they become dark colouring. The visualization can not be distinguished. Conversely the bare rock's contrast is stretching as shown in Fig. 2 (c) , the snowfield contrast becomes a small and brightness turns high, and on the optical image it changes into a wide expense of white colour. Simple enhanced disposal can only insist on the ground object of some kind, but other objects are blurred. In order to gain the ideal image contrast and brightness for all kinds of objects, one should extract some objects from images and then perform the contrast enhancement specially on them. This kind of processing can be done by means of the approaches for image analysis and pattern recognition.

In Antarctica area the ground objects are relatively simple. It is divided roughly into three kinds: the first kind is ice/snow area, which cover a large area, and it includs ice sheet, glacier, ice shelf, iceberg, etc.. The second kind is bare rock area with the exposed rocks and fresh water lakes, and there are no vegetation except little bryophyte and lichen. This area inclued mainly land-tied peninsula, islands and islets. The third kind is sea water. Their spectrum features are obvious and distinguished easily as shown in Fig. 3.

When we adopt maximum-likelihood classification algorithm (Schowengerdt, 1983) to recognize the patterns, the only two types (the bare rocks and sea water) was taken out. According to Bayes criterion, discriminate function for:

$$D_i(x)=P(x/i)P(i) \tag{5}$$

$$P(x/i)=\frac{1}{|\sum_i|^{(1/2)}(2\pi)^{k/2}}\exp[-1/2(X-\boldsymbol{M}_i)^{\mathrm{T}}\sum_i^{-1}(X-\boldsymbol{M}_i)] \tag{6}$$

Where $p(x/i)$ —condition probability density function

$\boldsymbol{M}_i$ — i kind's mean vector

$\sum_i$ — i kind's covariance matrix

$p(i)$ —priority probability

Adopting supervised classification (Swain and Daris, 1978) of statistic results of the

two types ground object's training sampling area, are as shown Table 2,3,4.

Table 2. Mean Value, standard deviation of training areas

	Bare rock			Sea water	
	Mean value	Standard deviation		Mean value	Standard deviation
TM5	85.92	21.46	TM5	3.98	0.89
TM4	57.56	10.98	TM4	8.60	2.09
TM3	73.22	13.42	TM3	16.36	3.48
TM2	53.92	9.38	TM2	21.96	2.98

The results of computer classification to examination of training areas was compared with practical ground objects, the confusing matrix (Swain and Daris,1978) are shown as Table 5. From the classification results, there are no confusing phenomenon between the bare rocks and sea water. The confusing between bare rocks and ice/snow arised from primarily remnant snow on the bare rocks. There are no confusing between the ice

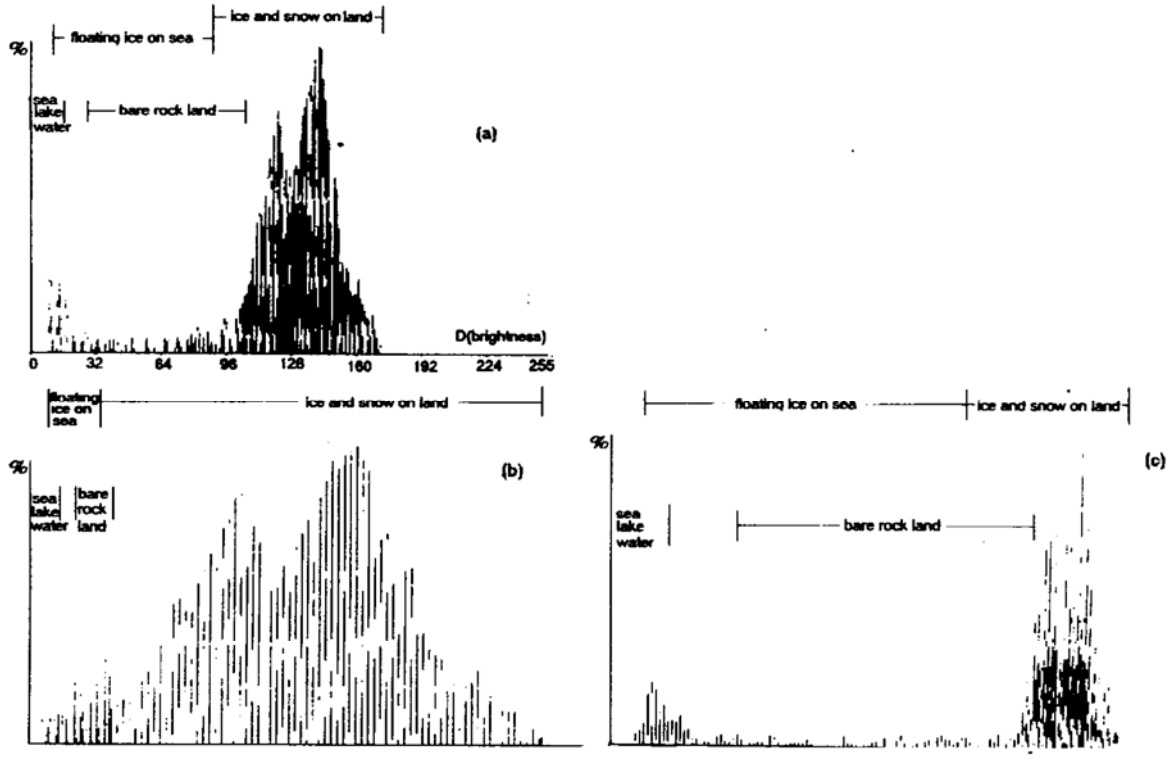

Fig. 2. Histogram before and after enhancement.

Table 3. Correlation coefficient between the bands

	Bare rock			Sea water			
	TM5	TM4	TM3		TM5	TM4	TM3
TM4	0.569			TM4	0.092		
TM3	0.339	0.913		TM3	0.096	0.874	
TM2	0.089	0.728	0.872	TM2	0.078	0.803	0.872

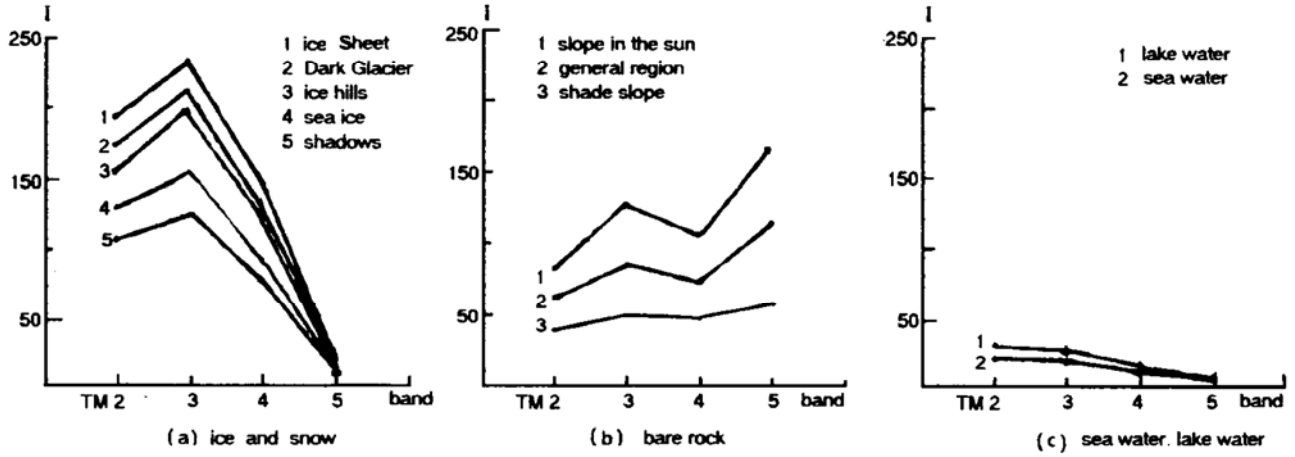

Fig. 3. Response spectral curves of three ground features in the Antarctic region.

sheet continent and sea water; the confusing between the sea water and ice/snow arised from the thawing sea ice that don't influence the contrast enhanced processing of part and whole image.

After taking out the bare rocks, linear contrast stretch (Hord,1982) was made:

$$d' = A \cdot d + B \qquad (7)$$

Where, d—On original image the bare rock's brightness value

d'—bare rocks after alone enhanced brightness value.

$A = (d_{max}' - d_{min}')/(d_{max} - d_{min})$

$B = -A \cdot d_{min} + d_{min}'$

Table 4. Covariance of image bands

	Bare rock					Sea water			
	TM5	TM4	TM3	TM2		TM5	TM4	TM3	TM2
TM5	460.339				TM5	0.797			
TM4	134.074	120.660			TM4	0.172	4.368		
TM3	97.567	134.583	180.189		TM3	0.298	6.359	12.123	
TM2	17.411	74.977	109.796	87.925	TM2	0.208	4.997	9.043	8.868

Table 5. Confusion matrix

Practical type \ Class type	Bare rock	Sea water
Bare rock	89.4	0
Sea water	0	95.4
Ice snow	10.6	4.6

The bare rock of the Zhongshan Station area, before and after making the contrast stretch, the brightness ranges are shown as Table 6.

Table 6. Grey level range before and after enhancement

Image \ Band	TM4		TM3		TM2	
	Min	Max	Min	Max	Min	Max
Original image	30	110	40	130	35	90
Enhancement image	84	170	120	240	100	200

The histogram based on proceeding contrast stretch of the bare rocks is shown in Fig. 4(a). The brightness of bare rock was very close with that of the ice/snow, the contrast changes small. Fig. 4(b) is the histogram that whole image has been divided into pieces and made linear stretch for every peice, both the bare rocks and ice/snow contrast was stretched, whose morphological details appeared very well. Owing to their different spectrum feature (show Fig. 3), TM4, TM3 and TM2 three bands have composed pseudo colour, bare rock is red, snow is pale blue, the sea water due to lower reflexive brightness on the three bands is more dark. Showing from Fig. 4(b), the floating thin ice area on the sea, whose brightness was very close to the sea water and it is black as well. In order to distinguish between the floating thin ice area and the sea water, the later has made for the blue of processing. The extracted sea water in Prydz Bay has been given respectively a value of brightnesson on three bands: blue: TM4⇒50, TM3⇒50,

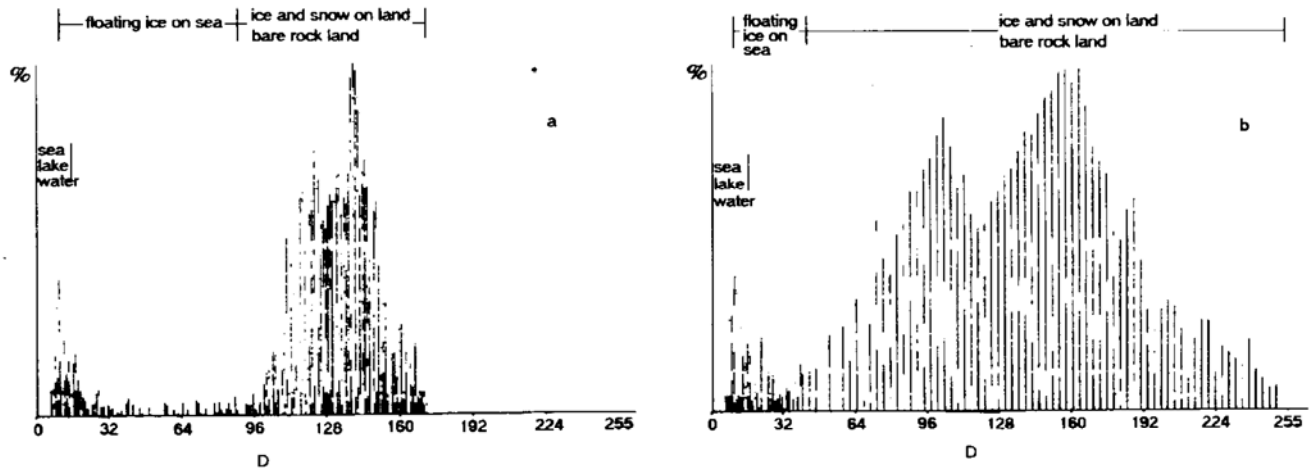

Fig. 4. The histogram based on image recognition after image enhancement.

TM2⇒200.

Now ocean has appeared bright blue, the colouring of whole image become coordinative, and a large floating thin ice area appear from the sea water. This should be useful to research distributing and melting characteristics of sea ice.

4 Digital rectifying of satellite image and mapping

TM images are a kind of two-dimensional image of many central projection that the satellite along track moving and the sensor left and right scanning to be produce. The

imaging equation (Wang, 1990) can be formulated as follows:

$$\begin{bmatrix} X \\ Y \\ Z \end{bmatrix}_P = \begin{bmatrix} X \\ Y \\ Z \end{bmatrix}_{St} + \lambda \mathbf{A}_t \mathbf{R}_\theta \begin{bmatrix} 0 \\ 0 \\ -f \end{bmatrix} \tag{8}$$

Where $[X,Y,Z]_P^T$ — geodetic coordinates of object point p

$[X,Y,Z]_{St}^T$ — geodetic coordinates of projection center

$\mathbf{A}_t$ — rotatory matrix of attitude angle

$\mathbf{R}_\theta$ — rotatory matrix of scanning angle.

The image has been roughly processed and most of systematic error has been eliminated. Remaining systematic error and random error are about 250 m. For setting image into map projection and going further into the image geometry precision, must be conducted. Rectifying function adopted twice polynomial disposal (Bahr, 1976) in clearing up nonlinear deformation.

$$\left.\begin{aligned} X &= A_0 + A_1 x + A_2 y + A_3 xy + A_4 x^2 + A_5 y^2 \\ Y &= B_0 + B_1 x + B_2 y + B_3 xy + B_4 x^2 + B_5 y^2 \end{aligned}\right\} \tag{9}$$

Where X,Y — geodectic coordinates of ground control point (UTM projection)

x,y — on image coordinates of the same point (the image line and row number)

A,B — polynomial transformation cofficient

Owing to lacking detailed and precise land map of 1 : 100000 over big scale about this area, therefore we took the ground control points of field survey. In 1989, according to the ground original point (Zhongshan Station) positioned by the satellite transit Doppler, we laid out four grade traverse net and surveyed obvious ground object points. Finally we selected seven ground control points. Because there were superfluous observations, it was necessary to adopt the least squares adjusting count (Konecny, 1976; Kratky, 1974). At first the error equation was established :

$$\left.\begin{aligned} \boldsymbol{V}_x &= \mathbf{K}\boldsymbol{A} - \boldsymbol{L}_x \\ \boldsymbol{V}_y &= \mathbf{K}\boldsymbol{B} - \boldsymbol{L}_Y \end{aligned}\right\} \tag{10}$$

Where $\mathbf{K} = \begin{bmatrix} 1 & X_1 & Y_1 & X_1 & Y_1 & X_1^2 & Y_1^2 \\ 1 & X_2 & Y_2 & X_2 & Y_2 & X_2^2 & Y_2^2 \\ \cdots & & & & & & \\ 1 & X_7 & Y_7 & X_7 & Y_7 & X_7^2 & Y_7^2 \end{bmatrix}$,

$\boldsymbol{A} = [A_0, A_1, \cdots, A_5]^T$,

$\boldsymbol{B} = [B_0, B_1, \cdots, B_5]^T$,

$\boldsymbol{L}_x = [x_1, x_2, \cdots, x_7]^T$,

$\boldsymbol{L}_y = [Y_1, Y_2, \cdots, Y_7]^T$

normal equations solved polynomial transformation coefficients:

$$\left.\begin{aligned} A&=(\mathbf{K}^{\mathrm{T}}\mathbf{K})^{-1}(\mathbf{K}^{\mathrm{T}}L_x)\\ B&=(\mathbf{K}^{\mathrm{T}}\mathbf{K})^{-1}(\mathbf{K}^{\mathrm{T}}L_y)\end{aligned}\right\} \tag{11}$$

the precision was evaluated:

$$\sigma=\pm\sqrt{\frac{[V^{T}V]}{m-f}} \tag{12}$$

Where m is the number of control points, f is the number of superfluous observation, total error and deviations of each point, as Table 7 shown, rectifying precisions accorded with the precision of the level position of point, and this 1 : 100000 map precision standard was made by China National Bureau of Surveying and Mapping.

Table 7. Deviations of control points in adjustment (unit:m).

	1	2	3	4	5	6	7	Total deviation
δx	−15.8	15.6	−19.8	19.4	2.9	−12.4	10.1	12.452285477
δy	24.3	−0.8	−7.6	−24.3	14.4	−3.0	−3.8	12.26208591

In rectifying process, the resampling problem occurs. The experiment used cubic convolution proceeding resample (Wang,1990). The lightness equation of inserting pixel as follows:

$$I_p=\mathbf{I}\otimes\mathbf{W} \tag{13}$$

Where I_p—lightness value of inserting pixel

$\mathbf{I}$ —lightness matrix of 4×4 region of neighboured inserting pixel

$\mathbf{W}$ —Weight matrix

$\otimes$ —operation symbol of space convolution

Weight matrix $\mathbf{W}$ makes use of sinc function to solve. $\mathrm{sinc}=\mathrm{sinc}(X/\Delta)=\frac{\sin(\pi X/\Delta)}{\pi X/\Delta}$, Usually $\Delta=1$, there is sinc function as follows equality:

$$\left.\begin{aligned} W_1(X_c)&=1-2X_c^2+|X_c|^3 && 0\leqslant|X_c|\leqslant1\\ W_2(X_c)&=4-8|X_c|+5X_c^2-|X_c|^3 && 1\leqslant|X_c|\leqslant2\\ W_3(X_c)&=0 && |X_c|\geqslant2\end{aligned}\right\} \tag{14}$$

When resample rectifying pixel size was selected to be 20m × 20m, so each interval 500 lines and 500 rows may arrange graticule of 10 km. For preventing negative coordinates, moved coordinate origin 500 km wesrward and 10000 km southward. Owing to using UTM projection in both the field control points and rectifying image, when arranged longitude and latitude lines, the data also transformed to UTM

coordinate. The transformation at follows:

$$\left.\begin{aligned} X &= 0.9996\left[S_m + \frac{\lambda^2 N}{2}\mathrm{Sin}\varphi\mathrm{Cos}\varphi + \frac{\lambda^4}{24}\mathrm{Sin}\varphi\mathrm{Cos}^3\varphi(5-\mathrm{tg}^2\varphi+9\eta^2+4\eta^4)+\cdots\right] \\ Y &= 0.9996\left[\lambda N\mathrm{Cos}\varphi + \frac{\lambda^3 N}{6}\mathrm{Cos}^3\varphi(1-\mathrm{tg}^2\varphi+\eta^2)+\frac{\lambda^5 N}{120}\mathrm{Cos}^5\varphi(5-18\mathrm{tg}^2\varphi+\mathrm{tg}^4\varphi)+\cdots\right] \end{aligned}\right\} \quad (15)$$

Because the images are each pixel image coordinates with line and row number therefore the coordinates must be reversed to line and row number, in the same way twice polynomial proceeding was adopted:

$$\left.\begin{aligned} L &= a_0 + a_1X + a_2Y + a_3XY + a_4X^2 + a_5Y^2 \\ P &= b_0 + b_1X + b_2Y + b_3XY + b_4X^2 + b_5Y^2 \end{aligned}\right\} \quad (16)$$

The satellite image-map of Larsemann Hills region in color is showed in inside back cover.

5 Conclusions

1. The direction filtering can efficiently remove the streaked noise.

2. Image enhancement seperatly with different areas by using the autometic recognition approach made the image clearly, and the details of the ice and snow surface become visible with reasonable contrast.

3. The precise processing used control points measured in the field, the mapping accuracy can fully satisfied the current National Standard of 1 : 100000 scale topographic map.

References

Bahr, H. P. (1976): Geometrical models for satellite scanner imagery. *Proceedings of 13th Corgr. ISP*, Helsinki.

Gonzalez, R. C. and Wintz, P. (1977): Digital image processing, *Reading Mass*, *Addison-Wesley.*

Hord, R. M. (1982): Digital image processing of remotely sensed data. Academic Press, London.

Konecny, G. (1976): Mathematical models and procedure for the geometric rectification of remote sensing imagery, *Proceedings of 14th congr. ISP*, Vol. XXI, part 3.

Kratky, V. (1974): Cartographic accuracy of ERTS, Photogrammetric Engineering. ASP.

Schowengerdt, R. A. (1983): Techniaues for image processing and classification in remote sensing. New York Academic Press.

Slater, P. N *et al.* (1975): Manual of remote sensing, ASP.

Swain, P. H. and Daris, S. M. (1978): Remote sensing: the quantitative approach. Mcgraw-Hill International Book Comp.

Wang Zhizhuo (1990): Principles of photogrammetry. press of Wuhan Technical University of Surveging and Mapping, Publishing House of Surveging and Mapping Beijing. P401～P433, P462～P515, P522～P534.